Synthesis of Oil-Dispersible Hexagonal-Phase and Hexagonal-Shaped $NaYF_4$:Yb,Er Nanoplates

Yang Wei, Fengqi Lu, Xinrong Zhang, and Depu Chen*

Department of Chemistry, Tsinghua University, Beijing 100084, People's Republic of China

Received March 14, 2006. Revised Manuscript Received July 20, 2006

Oil-dispersible α-$NaYF_4$ spherical nanoparticles and β-$NaYF_4$ hexagonal-shaped nanoplates were synthesized by the liquid−solid two-phase approach at different reaction temperatures. The TEM and FE-SEM images reveal that the nanoplates have a relatively narrow size distribution. In comparison with other methods, pure β-$NaYF_4$ hexagonal-shaped nanoplates were prepared under a relatively mild condition. The nanoplates grew at the liquid−solid interface with slow crystallization rate, which may be preferable for achieving β-$NaYF_4$.

Introduction

Upconversion luminescent materials have received great attention for a few decades.[1] Because of their unique anti-Stokes optical property, upconversion luminescent materials have a number of potential applications, including lasers,[2] three-dimensional displays,[3] light emitting devices,[4] biological detection,[5,6] and many others.[7] In recent years, several research groups have reported the upconversion luminescence in nanomaterials.[8−11] Besides the dried powdered nanocrystalline upconversion phosphors (UCPs), there is a growing interest to prepare UCPs that have a good dispersibility in organic solvents.[12−17] Spherical cubic-phase $NaYF_4$ nanoparticles that could be dispersed in nonpolar solvent have been prepared in homogeneous solution[13] and by a newly developed liquid−solid−solution (LSS) process.[15] Very recently, the methods to prepare $NaYF_4$:Yb,Er/Tm nanocrystals based on the co-thermolysis of sodium trifluoroacetate and rare earth trifluoroacetate were independently reported by Yan et al.[16] and Capobianco et al.[17] $NaYF_4$ exists in two polymorphs at ambient pressure: cubic α-phase and hexagonal β-phase. β-$NaYF_4$ has been reported as the most efficient host material for green and blue UCPs.[18] In our previous research,[6] the cubic-to-hexagonal phase transition process of $NaYF_4$ is an exothermic process. Correspondingly, the hexagonal-to-cubic phase transition process of $NaYF_4$ has been reported as an endothermic process.[18] From the results provided by differential scanning calorimetric measurement, it is reasonable to conclude that for $NaYF_4$, the hexagonal phase is more thermodynamically stable than the cubic phase. However, in most cases for preparation of $NaYF_4$, α-$NaYF_4$ nanocrystals were obtained. The cubic phase could transfer into hexagonal phase under heat treatment. Annealing treatment[18] and hydrothermal or solvothermal treatment[19,20] were adopted to produce the β-$NaYF_4$. β-$NaYF_4$ could also be formed under drastic conditions reported by Yan et al.[16] In this paper, a liquid−solid two-phase approach was used to synthesize β-$NaYF_4$ directly. The results revealed that not only β-$NaYF_4$ hexagonal-shaped nanoplates but also α-$NaYF_4$ spherical nanoparticles could be synthesized by the liquid−solid two-phase approach at different reaction temperatures. The possible mechanism was discussed in this paper.

Experimental Section

Materials. Sodium fluoride (NaF), sodium hydroxide (NaOH), ethanol, and hydrochloric acid (HCl) were obtained from Beijing Chemical Corp. (Beijing, China). Yttrium oxide (Y_2O_3, 99.99%), ytterbium oxide (Yb_2O_3, 99.99%), and erbium oxide (Er_2O_3, 99.99%) were obtained from Grirem Advanced Materials Co., Ltd. (Beijing, China), and were of SpecPure grade. Oleic acid was

* To whom correspondence should be addressed. Tel.: +86 10 62781691. Fax: +86 10 62782485. E-mail: chendp@chem.tsinghua.edu.cn.

(1) Auzel, F. *Chem. Rev.* **2004**, *104*, 139.
(2) Scheps, R. *Prog. Quantum Electron.* **1996**, *20*, 271.
(3) Downing, E.; Hesselink, L.; Ralston, J.; Macfarlane, R. *Science* **1996**, *273*, 1185.
(4) Sivakumar, S.; van Veggel, F. C. J. M.; Raudsepp, M. *J. Am. Chem. Soc.* **2005**, *127*, 12464.
(5) van de Rijke, F.; Zijlmans, H.; Li, S.; Vail, T.; Raap, A. K.; Niedbala, R. S.; Tanke, H. J. *Nat. Biotechnol.* **2001**, *19*, 273.
(6) Yi, G. S.; Lu, H. C.; Zhao, S. Y.; Yue, G.; Yang, W. J.; Chen, D. P.; Guo, L. H. *Nano Lett.* **2004**, *4*, 2191.
(7) Shalav, A.; Richards, B. S.; Trupke, T.; Kramer, K. W.; Gudel, H. U. *Appl. Phys. Lett.* **2005**, *86*, 013505.
(8) Yi, G. S.; Sun, B. Q.; Yang, F. Z.; Chen, D. P.; Zhou, Y. X.; Cheng, J. *Chem. Mater.* **2002**, *14*, 2910.
(9) Matsuura, D. *Appl. Phys. Lett.* **2002**, *81*, 4526.
(10) Patra, A.; Friend, C. S.; Kapoor, R.; Prasad, P. N. *J. Phys. Chem. B* **2002**, *106*, 1909.
(11) Vetrone, F.; Boyer, J. C.; Capobianco, J. A.; Speghini, A.; Bettinelli, M. *J. Phys. Chem. B* **2003**, *107*, 1107.
(12) Heer, S.; Lehmann, O.; Haase, M.; Gudel, H. U. *Angew. Chem., Int. Ed.* **2003**, *42*, 3179.
(13) Heer, S.; Kompe, K.; Gudel, H. U.; Haase, M. *Adv. Mater.* **2004**, *16*, 2102.
(14) Yi, G. S.; Chow, G. M. *J. Mater. Chem.* **2005**, *15*, 4460.
(15) Wang, X.; Zhuang, J.; Peng, Q.; Li, Y. D. *Nature* **2005**, *437*, 121.
(16) Mai, H. X.; Zhang, Y. W.; Si, R.; Yan, Z. G.; Sun, L. D.; You, L. P.; Yan, C. H. *J. Am. Chem. Soc.* **2006**, *128*, 6426.
(17) Boyer, J. C.; Vetrone, F.; Cuccia, L. A.; Capobianco, J. A. *J. Am. Chem. Soc.* **2006**, *128*, 7444.
(18) Kramer, K. W.; Biner, D.; Frei, G.; Gudel, H. U.; Hehlen, M. P.; Luthi, S. R. *Chem. Mater.* **2004**, *16*, 1244.
(19) Wang, L. Y.; Yan, R. X.; Hao, Z. Y.; Wang, L.; Zeng, J. H.; Bao, H.; Wang, X; Peng, Q.; Li, Y. D. *Angew. Chem., Int. Ed.* **2005**, *44*, 6054.
(20) Zeng, J. H.; Su, J.; Li, Z. H.; Yan, R. X.; Li, Y. D. *Adv. Mater.* **2005**, *17*, 2119.

10.1021/cm0606171 CCC: $33.50
Published on Web 10/25/2006

purchased from Beijing Chemical Reagents Co. (Beijing, China). 1-Octadecene was purchased from Acros Organics (NJ). Rare earth chlorides ($RECl_3 \cdot 6H_2O$ with RE = Y, Yb, Er) were prepared by dissolving the corresponding rare earth oxides in hydrochloric acid at elevated temperature, and then evaporating the solvent in a vacuum. Sodium oleate was prepared by reacting oleic acid and sodium hydroxide using ethanol as reaction medium. Sodium hydroxide was dispersed in ethanol under vigorous stirring, and then equal molar oleic acid was added dropwise. After the neutralization reaction was completed, ethanol and water were evaporated in a vacuum.

Synthesis of Rare Earth Oleate Complexes. A literature method for the synthesis of iron−oleate complex[21] was adopted to prepare the rare earth oleate complexes. In a typical synthesis of yttrium−oleate complex, 20 mmol of yttrium chloride ($YCl_3 \cdot 6H_2O$) and 60 mmol of sodium oleate were dissolved in a mixture solvent composed of 40 mL of ethanol, 30 mL of distilled water, and 70 mL of hexane. The resulting solution was added into a 250-mL round-bottomed flask with a reflux condenser, and then heated to 70 °C and kept at that temperature for 4 h. After the reaction was completed, the reaction mixture was transferred into a separatory funnel. The upper organic layer was separated and washed three times with 30 mL of distilled water. After being washed, yttrium−oleate complex was produced in a waxy solid form by evaporating off the remaining hexane. Ytterbium−oleate complex and erbium−oleate complex were synthesized in the same way.

Synthesis of $NaYF_4$:Yb,Er Nanocrystals. The reaction temperature is the only difference between the synthetic procedures for preparation of α-$NaYF_4$:Yb,Er spherical nanoparticles and β-$NaYF_4$:Yb,Er hexagonal-shaped nanoplates. For the synthesis of β-$NaYF_4$:Yb,Er hexagonal-shaped nanoplates, 0.2 g of NaF solid powder and 30 mL of 1-octadecene were added into a 100 mL three-necked flask, and NaF was dispersed in the 1-octadecene with vigorous magnetic stirring. The mixture was degassed under vacuum for about 30 min, and flushed periodically with N_2. The temperature of the reaction flask was then stabilized at 260 °C under N_2 atmosphere. Next, 0.8 mmol of yttrium−oleate complex, 0.17 mmol of ytterbium−oleate complex, and 0.03 mmol of erbium−oleate complex were dissolved in 30 mL of 1-octadecene to form an optically transparent solution. This solution was bubbled with N_2 gas for 10 min, and then was quickly delivered to the vigorously stirring reaction flask in a single injection with a 50-mL syringe through a rubber septum. The reaction was kept at 260 °C for 6 h in N_2 atmosphere under vigorous stirring. As the reaction mixture was cooled to ∼60 °C, it was washed three times with 30 mL of ∼60 °C hot deionized water in a separatory funnel. Next, 100 mL of ethanol was added to the resulting solution containing the nanocrystals. The nanocrystals were separated by centrifugation. The as-prepared nanocrystals could be easily redispersed in various nonpolar organic solvents, such as hexane and toluene. When the reaction temperature was lowered to 210 °C, α-$NaYF_4$:Yb,Er spherical nanoparticles were obtained.

Characterization. Investigations on the size and morphology of the nanocrystals were performed using a JEM-1200EX transmission electron microscope (TEM) (JEOL, Japan) operating at accelerating voltages up to 100 kV and a JSM-7401F field emission scanning electron microscope (FE-SEM) (JEOL, Japan) operating at accelerating voltages up to 1 kV. Powder X-ray diffraction patterns were obtained on a D/max-RB X-ray diffractometer (Rigaku, Japan) and a D/max-2500 X-ray diffractometer (Rigaku, Japan). Upconversion fluorescent spectra were measured on a LS-55 fluorescence spectrophotometer (Perkin-Elmer Corp.) with an external 980 nm laser (Beijing Hi-Tech Optoelectronic Co., China) instead of internal excitation source. A 62.5/125 (core/cladding dimensions, which are given in micrometers) multimode optical fiber with the numerical aperture 0.22 was used to conduct the laser into the spectrophotometer. The distance between the fiber head and the samples is about 3 mm.

(21) Park, J.; An, K. J.; Hwang, Y. S.; Park, J. G.; Noh, H. J.; Kim, J. Y.; Park, J. H.; Hwang, N. M.; Hyeon, T. *Nat. Mater.* **2004**, *3*, 891.

Results and Discussion

Synthesis of $NaYF_4$:Yb, Er Nanocrystals. A liquid−solid two-phase approach was used to synthesize the $NaYF_4$:Yb,Er nanocrystals. Because of its high boiling point, 1-octadecene was chosen as the solvent for the high-temperature growth and annealing of $NaYF_4$ crystallites. Rare earth oleate complexes were dissolved in the organic solvent as the liquid phase. Because of the insolubility of NaF in 1-octadecene, NaF was dispersed in the same organic solvent as the solid phase. $NaYF_4$:Yb,Er nanocrystals grew at the liquid−solid interface, and oleic acid released from the rare earth oleate complexes could bind to the growing nanocrystals with the alkyl chains outward, through which the nanocrystals gained hydrophobic surfaces.

TEM was used to map the shape and size of the nanocrystals dispersed on a carbon-coated copper grid from hexane solutions, and FE-SEM was also used to give the three-dimensional morphological observation of the nanocrystals. The TEM images of the nanocrystals prepared at 210, 230, and 260 °C are shown in Figure 1A,B and Figure 2, respectively. The TEM images with higher magnification for these nanocrystals are shown in Figures S1−S3. As shown in Figure 1A and Figure S1, the nanoparticles obtained at 210 °C have roughly spherical shapes with the average size of about 7 nm. Increasing the reaction temperature to 230 °C, much bigger nanocrystals were formed. It could be found from the TEM images shown in Figure 1B and Figure S2 that the shapes of these nanocrystals are between round and hexagonal. In fact, from the FE-SEM image shown in Figure S5, it is clear that the nanocrystals obtained at 230 °C were mixtures composed of hexagonal-shaped nanoplates and small nanoparticles glued to the nanoplates. After the reaction temperature reached 260 °C, pure hexagonal-shaped nanoplates were obtained. The TEM images of these nanoplates were shown in Figure 2 and Figure S3, and the FE-SEM images of them were shown in Figure S6. The TEM images shown in Figure 2 reveal that most of the nanoplates are lying flat on the face, and a small quantity of the nanoplates are standing on the edge. The edge lengths of the nanoplates shown in the TEM images are not equal, which is probably due to the nanocrystals being tilted by different angles with respect to the carbon films. The nanoplates are characterized by ∼35 nm in edge length and ∼20 nm in thickness. The TEM and FE-SEM images reveal that the nanoplates have a relatively narrow size distribution. In the liquid−solid two-phase approach, both nucleation and growth of nanoplates could only occur at the interface of the two phases. After the nuclei formed at the interface, they could enter the liquid phase, and thus the nanocrystals stopped growing. Only if the nanocrystals returned to the interface could they continue to grow. The bigger size nanocrystals had, the more slowly they moved. Smaller

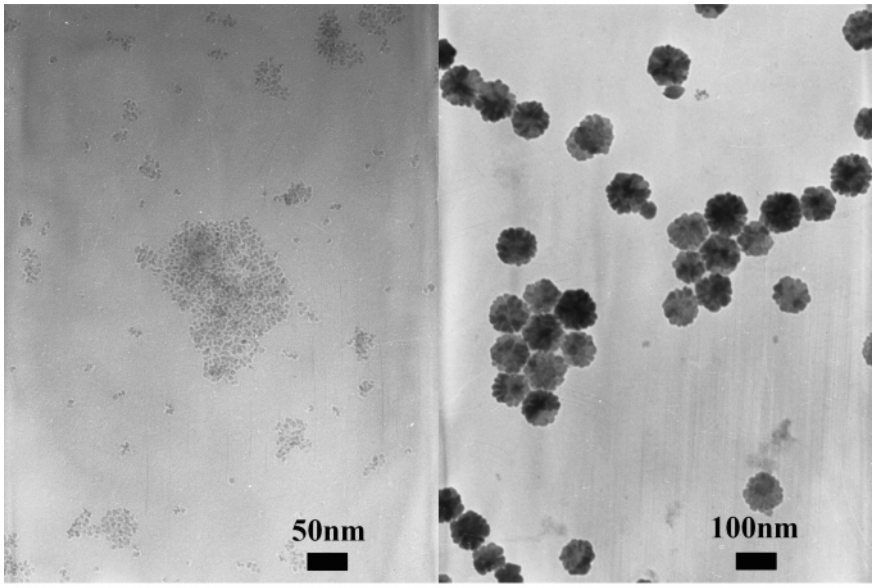

Figure 1. TEM images of $NaYF_4$:Yb,Er nanocrystals obtained at 210 °C (A) and 230 °C (B).

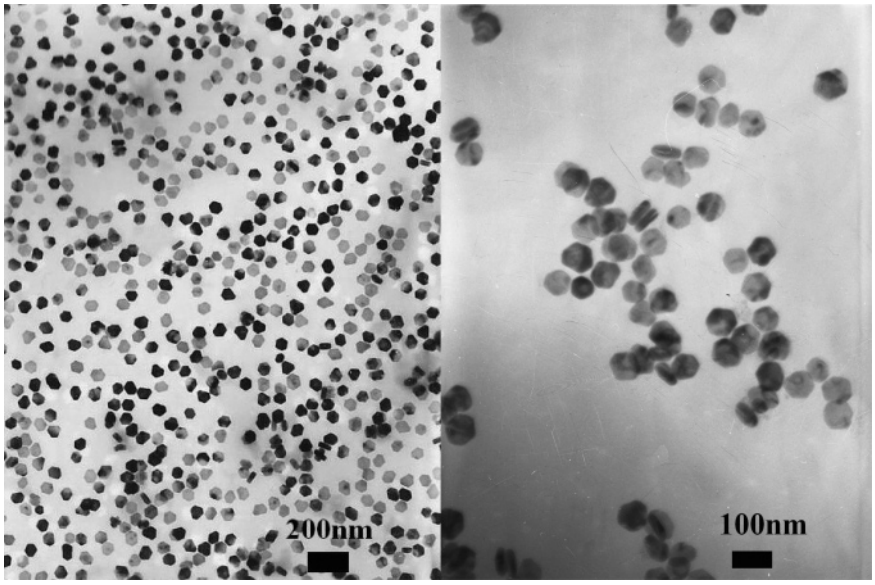

Figure 2. TEM images of β-$NaYF_4$:Yb,Er nanoplates obtained at 260 °C.

nanocrystals could move into the liquid phase and went back to the interface more quickly than bigger nanocrystals, and so the smaller nanocrystals had more chance to grow than the bigger nanocrystals; thus the narrow particle size distribution was obtained.

The efficiency of the reaction that occurred at the liquid−solid interface is much lower than that in homogeneous solution. Several factors, such as the reaction time, stirring speed, reaction temperature, have strong impacts on the output of this reaction. Vigorous stirring and enough high reaction temperature were required. To avoid the thermolysis of rare earth oleate complexes at high temperature, the reaction temperature for preparation of hexagonal-shaped nanoplates was chosen at 260 °C. The output of the reaction increased greatly with increasing the reaction time. From the TEM images shown in Figure S4, there were no obvious difference found in the size and morphology of the nanoplates obtained from different reaction time. This result could be good evidence for the reaction mechanism provided above.

The XRD results reveal that the spherical $NaYF_4$ nanoparticles synthesized at 210 °C crystallized in the cubic α-phase and the hexagonal-shaped $NaYF_4$ nanoplates synthesized at 260 °C crystallized in the hexagonal β-phase. The crystallographic phase of the initial seed during the nucleation processes is critical for directing the nanocrystal shapes due to its characteristic unit cell structure.[22] The cubic α-$NaYF_4$ seeds have isotropic unit cell structures, which generally induce the isotropic growth of nanocrystals, and therefore spherical α-$NaYF_4$ nanoparticles were observed. In contrast, hexagonal β-$NaYF_4$ seeds have anisotropic unit cell structures, which can induce anisotropic growth along crystallographically reactive directions, and thus hexagonal-shaped nanoplates were obtained.

Structural Characterization of $NaYF_4$:Yb,Er Nanocrystals. X-ray powder diffraction patterns of $NaYF_4$:Yb,-

(22) Jun, Y. W.; Lee, J. H.; Choi, J. S.; Cheon, J. *J. Phys. Chem. B* **2005**, *109*, 14795.

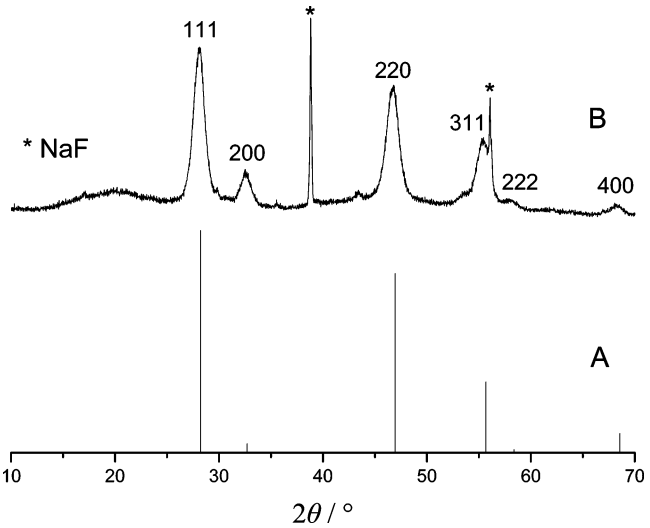

Figure 3. Calculated line pattern (A) and experimental powder XRD data (B) for the α-$NaYF_4$:Yb,Er nanoparticles obtained at 210 °C.

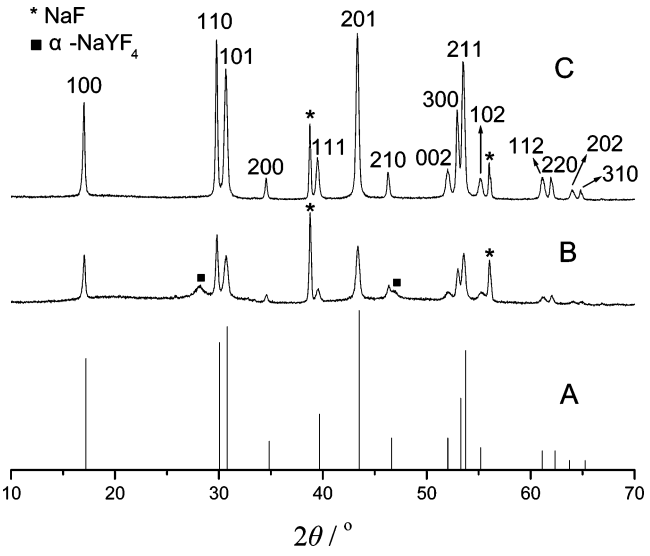

Figure 4. Calculated line pattern (A) and experimental powder XRD data for the β-$NaYF_4$:Yb,Er nanoplates obtained at 230 °C (B) and 260 °C (C).

Er nanocrystals obtained at 210, 230, and 260 °C are shown in Figure 3 and Figure 4. Deduced from the XRD data, all of the samples were well-crystallized. Except two peaks that were marked with asterisks, all of the other peaks of the nanoparticles prepared at 210 °C and of the nanoplates prepared at 260 °C could be readily indexed to the cubic α-$NaYF_4$ phase or hexagonal β-$NaYF_4$ phase, respectively. For the sample synthesized at 230 °C, the β-$NaYF_4$ phase was the major species; however, a small quantity of α-$NaYF_4$ phase could be detected. The selected-area electron diffraction (SAED) patterns shown in Figure S7, which were taken from a single nanoplate obtained at 260 °C, demonstrated the single-crystalline nature of the sample; it could be readily indexed as hexagonal phase, in good agreement with its XRD data.

The average particle size estimated by line-broadening was 6.4 nm for the α-$NaYF_4$ spherical nanoparticles. For β-$NaYF_4$ hexagonal-shaped nanoplates, the particle sizes estimated by line-broadening from different diffraction peaks varied from 26.2 to 63.2 nm.

These two asterisked peaks in the XRD patterns could be well indexed to the reactant NaF, which means the nanocrystals obtained were mixed with some residual NaF. During the reaction process, the polar head of oleic acid could absorb to the NaF particles with the nonpolar tail on the outside, through which the NaF particles gained hydrophobic surfaces. After the reaction was completed, to remove the residual NaF, the reaction mixture was washed three times with deionized water in a separatory funnel; however, it seemed that this procedure is not effective enough to remove all of the residual NaF. NaF could be removed completely from the products; the detailed procedure is described in the Supporting Information.

For bulk $NaYF_4$, α-phase is the metastable high-temperature phase, while β-phase is the thermodynamically stable low-temperature phase.[16] At temperatures above approximately 700 °C, the β-phase is unstable.[18] However, in most cases for preparation of nanosized $NaYF_4$, it tends to crystallize in the cubic phase, the less thermodynamically stable phase, first. In their newly reported work, Yan et al. demonstrated a general one-step synthesis of $NaREF_4$ (RE = Pr to Lu, Y) nanocrystals via the co-thermolysis of Na(CF_3COO) and RE(CF_3COO)$_3$ precursors.[16] Pure α-$NaYF_4$ could be obtained at a low temperature (280 °C) and a low ratio of Na/RE with a relatively short reaction time, while β-$NaYF_4$ was formed only under drastic conditions (high Na/RE, 330 °C, and long reaction time).

It is interesting that both pure α-$NaYF_4$ nanocrystals and β-$NaYF_4$ nanoplates could be obtained in this liquid−solid two-phase approach, and the only difference between the synthetic procedures is the reaction temperature. In comparison with the method to prepare the α-$NaYF_4$ spherical nanoparticles in homogeneous solution,[13] the liquid−solid−solution (LSS) process,[15] and the thermal decomposition method,[16,17] the reaction rate and crystallization rate are much slower in the liquid−solid two-phase approach, for both nucleation and growth of nanocrystals could only occur at the liquid−solid interface. To overcome the energy barrier for the formation of β-$NaYF_4$, appropriate high temperature was needed to prepare β-$NaYF_4$. It is why only α-$NaYF_4$ nanoparticles were obtained at 210 °C and mixtures composed of β-$NaYF_4$ hexagonal-shaped nanoplates and α-$NaYF_4$ spherical nanoparticles were obtained at 230 °C in this approach. Pure β-$NaYF_4$ hexagonal-shaped nanoplates could be obtained at 260 °C, a relatively mild condition, in this liquid−solid two-phase approach. In contrast, drastic conditions were needed for synthesis of β-$NaYF_4$ via the thermal decomposition method. In addition, in a glycerol-mediated synthesis of $NaYF_4$:Yb,Er nanoparticles in homogeneous solution at 260 °C, pure α-$NaYF_4$ was obtained even after 6 h of reaction. However, pure hexagonal phase was detected in the products obtained after 2 h of reaction via the liquid−solid two-phase approach. (The details are described in the Supporting Information.)

In the structure of α-$NaYF_4$, the cation sites are occupied randomly by Na^+ and Y^{3+} cations, while in β-$NaYF_4$ the cation sites are of three types: a 1-fold site occupied by Y^{3+}, a 1-fold site occupied randomly by $^1/_2Na^+$ and $^1/_2Y^{3+}$, and a 2-fold site occupied randomly by Na^+ and vacancies. Thus,

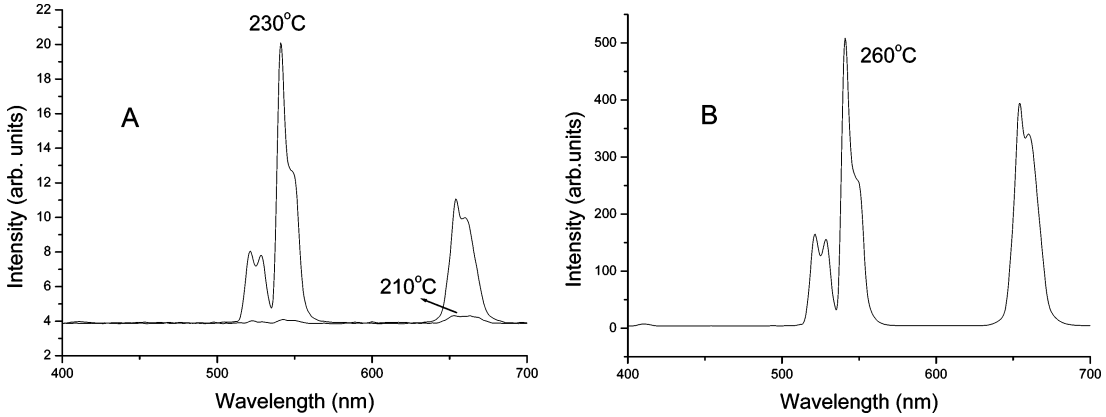

Figure 5. Upconversion emission spectrum of $NaYF_4$:Yb,Er nanocrystals obtained at 210, 230, and 260 °C (the excitation conditions were the same for these samples: the laser power is 437 mW, and the emission slit is 3 nm).

for $NaYF_4$, the cubic-to-hexagonal phase transformation is of a disorder-to-order character with respect to cations.[16] From the results described above, we presume that a slow crystallization process may be preferable for achieving β-$NaYF_4$, the order phase. A similar phenomenon was found in the recently reported synthesis of lanthanide fluoride nanoparticles by a reverse microemulsion method.[23] Spherical amorphous YF_3 particles were obtained by the classical microemulsion method (mixing of two microemulsions containing fluoride and YCl_3, respectively); conversely, single-crystal particles with regular hexagonal and triangular shape were obtained by the single microemulsion method (direct addition of a fluoride solution to a microemulsion containing YCl_3). The particle growth and crystallization were slower in the single microemulsion method than in the classical microemulsion method, and, as a result, single-crystal nanoparticles rather than the amorphous particles were obtained in the single microemulsion.

Upconversion Fluorescent Properties of β-$NaYF_4$:Yb,Er Nanoplates. Room-temperature upconversion fluorescence spectra of $NaYF_4$:Yb,Er nanocrystals obtained at 210, 230, and 260 °C in the wavelength region of 400−700 nm are shown in Figure 5. As compared to the fluorescent intensity of α-$NaYF_4$ nanoparticles prepared at 210 °C, that of β-$NaYF_4$ nanoplates prepared at 260 °C is enhanced greatly. This result is in good agreement with the reported result that β-$NaYF_4$ is the most efficient host material for green and blue upconversion phosphors known today.[18−20] It should be pointed out that the enhancement of the fluorescent intensity may be partly due to the increase of the particle size. There are three major bands in the curve, centered at 522, 542, and 654 nm, respectively. The mechanisms responsible for the upconversion fluorescence are shown in the Supporting Information.

The 542 nm-to-654 nm emission ratio of β-$NaYF_4$ nanoplates prepared at 260 °C is about 1.29 to 1. Several factors such as doping levels, excitation power, and impurities have impacts on the green-to-red emission ratio. In this paper, the doping levels for Yb^{3+} and Er^{3+} were not optimized. The actual molar ratio of the rare earth metals (Y:Yb:Er) in the β-$NaYF_4$ nanoplates obtained at 260 °C examined by ICP-OES was 0.816:0.156:0.028. This result is in good agreement with the planned molar ratios for Y, Yb, and Er (0.80:0.17:0.03). Furthermore, the organic capping groups binding on the surface of the β-$NaYF_4$ nanoplates may increase the multiphonon relaxation rates between the metastable states, which reduce the green-to-red emission ratio.

Acknowledgment. Financial support from National Nature Science Foundation of China (20535020) is gratefully acknowledged.

Supporting Information Available: TEM and FE-SEM images of $NaYF_4$:Yb,Er nanocrystals, SAED and XRD patterns of β-$NaYF_4$:Yb,Er nanoplates obtained at 260 °C, procedures for removing residual NaF from products, brief description for the glycerol-mediated synthesis of α-$NaYF_4$:Yb,Er nanoparticles, and mechanisms responsible for the upconversion fluorescence of β-$NaYF_4$:Yb,Er nanoplates obtained at 260 °C (PDF). This material is available free of charge via the Internet at http://pubs.acs.org.

(23) Lemyre, J. L.; Ritcey, A. M. *Chem. Mater.* **2005**, *17*, 3040.

CM0606171